HHS Public Access

Author manuscript

Biomaterials. Author manuscript; available in PMC 2017 February 01.

Published in final edited form as:

Biomaterials. 2016 February ; 80: 11–19. doi:10.1016/j.biomaterials.2015.11.065.

Biomaterials Transforming growth factor-beta 1 delivery from microporous scaffolds decreases inflammation post-implant and enhances function of transplanted islets

JMH Liu[1,2], **J Zhang**[3], **X Zhang**[4], **KA Hlavaty**[3], **CF Ricci**[5], **JN Leonard**[5], **LD Shea**[2,6], and **RM Gower**[7,8]

[1]Interdisciplinary Biological Sciences Program, Northwestern University, Evanston, IL, 60208, USA

[2]Department of Biomedical Engineering, University of Michigan, Ann Arbor, MI, 48109, USA

[3]Department of Biomedical Engineering, Northwestern University, Evanston, IL, 60208, USA

[4]Department of Surgery, Division of Transplantation, Feinberg School of Medicine, Northwestern University, Chicago, IL 60611, USA

[5]Department of Chemical and Biological Engineering, Northwestern University, Evanston, IL, 60208, USA

[6]Department of Chemical Engineering, University of Michigan, Ann Arbor, MI, 48109, USA

[7]Department of Chemical Engineering, University of South Carolina, Columbia, SC, 29208, USA

[8]Biomedical Engineering Program, University of South Carolina, Columbia, SC, 29208, USA

Abstract

Biomaterial scaffolds are central to many regenerative strategies as they create a space for infiltration of host tissue and provide a platform to deliver growth factors and progenitor cells. However, biomaterial implantation results in an unavoidable inflammatory response, which can impair tissue regeneration and promote loss or dysfunction of transplanted cells. We investigated localized TGF-β1 delivery to modulate this immunological environment around scaffolds and transplanted cells. TGF-β1 was delivered from layered scaffolds, with protein entrapped within an inner layer and outer layers designed for cell seeding and host tissue integration. Scaffolds were implanted into the epididymal fat pad, a site frequently used for cell transplantation. Expression of cytokines TNF-a, IL-12, and MCP-1 were decreased by at least 40% for scaffolds releasing TGF-β1 relative to control scaffolds. This decrease in inflammatory cytokine production corresponded to a 60% decrease in leukocyte infiltration. Transplantation of islets into diabetic mice on TGF-β1

*Corresponding Authors: Prof. Lonnie D. Shea, Department of Biomedical Engineering, The University of Michigan, 1119 Carl A. Gerstacker Building, 2200 Bonisteel Boulevard, Ann Arbor, MI 48109, Phone: (734) 764-7149, Fax: (734) 936-1905, ldshea@umich.edu. Prof. R. Michael Gower, Department of Chemical Engineering, University of South Carolina, Swearingen Engineering Center, Room 2C21, 301 Main Street, Columbia, SC, 29108, Phone: (803) 777-1541, Fax: (803) 777-0973, gowerrm@mailbox.sc.edu.

scaffolds significantly improved the ability of syngeneic islets to control blood glucose levels within the first week of transplant and delayed rejection of allogeneic islets. Together, these studies emphasize the ability of localized TGF-β1 delivery to modulate the immune response to biomaterial implants and enhance cell function in cell-based therapies.

Keywords

immunoengineering; immunomodulation; transplant; scaffold; leukocyte

Introduction

Cell transplantation holds tremendous potential for regenerative strategies such as those focused on the heart [1], liver [2], nervous system [3], and diabetes [4]; however, cell survival following transplantation and long-term function pose significant hurdles for these therapies. To address these issues, biomaterial scaffolds designed to enhance cell survival, engraftment, and function at the implant site have been the focus of intense investigation [5–7]. Biomaterials have been modified with biological signals, such as extracellular matrix proteins to modulate cell adhesion and migration, or inductive factors to stimulate cell survival, proliferation, or differentiation. The ultimate goal of these modifications is to create an environment within the implant site that will promote engraftment and long-term function of the transplanted cells.

Despite biological cues presented by the scaffold, tissue damage due to surgery and implantation evokes inflammation that will drastically alter the immune environment within the implant and can adversely affect the short- and long-term survival and function of transplanted cells. Tissue resident macrophages detect tissue damage through pattern recognition receptors leading to the release of inflammatory proteins such as tumor necrosis factor-alpha (TNF-a), interlukin-1beta (IL-1β), and chemokines that recruit neutrophils [8]. TNF-a, IL-1β, and IL-17, released by neutrophils, induce expression of monocyte chemotactic protein-1 (MCP-1) by tissue resident cells including fibroblasts, endothelial cells, and smooth muscle cells, leading to the recruitment of monocytes, dendritic cells (DCs), and natural killer (NK) cells. Neutrophils and NK cells can release reactive oxygen species, enzymes, and cytolytic factors that can damage endogenous and transplanted cells, irrespective of whether transplanted cells are autologous or allogeneic; however, if the transplanted cells are allogeneic, DCs will activate T and B cells known to play critical roles in transplant rejection [9–14]. In this way, simply implanting allogeneic tissue initiates an inflammatory cascade that leads to its destruction. Thus, an ability to reduce local inflammation and promote non-activated or tolerogenic immune cell phenotypes during and immediately after implant has the potential to enhance both autologous and allogeneic cell-based regenerative therapies.

In this study, we investigated poly-lactide-co-glycolide (PLG) scaffolds designed to release recombinant transforming growth factor-beta1 (TGF-β1) in order to modulate the local immune environment. Localized delivery of immunomodulatory factors is emerging as a strategy for controlling the immune environment within the implant site. TGF-β1 has a

substantial role in innate immunity, regulating the recruitment, activation, and function of neutrophils, macrophages, and NK cells [15]. Furthermore, TGF-β1 antagonizes antigen presentation and maturation of DCs [16, 17] and promotes the differentiation of naïve CD4+ T cells into regulatory T cells (Tregs) [18]. Thus, we hypothesized that TGF-β1 release from biomaterial scaffolds could decrease inflammation within the implant, enhance function of syngeneic cell transplants and delay immune rejection of allogeneic cells. This hypothesis was investigated using PLG scaffolds that support islet transplantation into the epididymal fat pad of diabetic mice [19–23], a model that allows for non-invasive monitoring of cell viability and function by measurement of blood glucose levels. Major objectives were to quantify the effect of TGF-β1 delivery on the inflammatory environment within the implant site and correlate these effects with the ability of the transplanted islets to establish and maintain euglycemia in diabetic animals.

Materials and Methods

Scaffold fabrication

Protein-loaded poly(lactide-co-glycolide) (PLG) scaffolds were fabricated using a previously described gas foaming and particulate leaching process [24], with a modified design containing a non-porous center layer for protein loading. PLG (75:25 mol ratio d,l-lactide to glycolide, 0.76 dL/g) (Lakeshore Biomaterials) was dissolved in dichloromethane to make either a 2% or 6% (w/w) solution, which was then emulsified in 1% poly(vinyl alcohol) to create microspheres. The microspheres were collected by centrifugation, washed with deionized water, and lyophilized overnight. The non-porous center layer for TGF-β1 scaffolds was made by reconstituting 2 mg of 2% PLG microspheres in sterile deionized water containing 1mg of mannitol (Sigma) and recombinant murine TGF-β1 (Cell Signaling Technology). The mixture was lyophilized and compressed into a 3 mm diameter disk with a height of 100 μm using a manual KBr pellet hand press (Pike Technologies). Center layers for the control scaffolds were made using the same procedures while omitting protein from the lyophilized mixture. The composite scaffold was constructed by sandwiching the protein-containing non-porous layer between two porous layers containing 6% PLG microspheres and NaCl particles 250–425 μm diameter combined in a 1:30 ratio. The three layers were pressed together in a 5 mm steel die at 1500 pounds per square inch using a Carver press into a 5 mm diameter disk with a height of 2 mm. The scaffold was then gas-foamed after equilibration to 800 psi under CO_2 gas in a custom-made pressure vessel. Salt particles were removed from the foamed scaffolds by immersion in 10 mL deionized water for 1 hour.

In vitro TGF-β1 Release Assay

Scaffolds were leached in 10 mL of water containing 1% BSA (fraction V, protease free, Millipore) for 1 hour to remove salt porogen and were then transferred into 1mL of EBSS (Life Technologies) containing 1% BSA, penicillin, and streptomycin and incubated at 37°C for 28 days with gentle agitation. At 1, 3, 7, 14, 21, and 28 days scaffolds were placed in fresh EBSS and the old EBSS was frozen. At the end of the experiment TGF-β1 was measured using a TGF-β1 DuoSet® ELISA Kit (R&D Systems) as per the manufacturer's instructions.

Scaffold implantation

Prior to implant, scaffolds were disinfected in 70% ethanol and then washed twice in sterile phosphate buffered saline (PBS; Life Technologies). For non-transplant studies, mice received scaffold implants into both epididymal fat pads for a total of two per mouse. Scaffold implantation was performed as previously described [25]. Prior to implant, recipient mice were anesthetized with an intraperitoneal injection of ketamine (10 mg/kg) and xylazine (5 mg/kg), and the abdomen was shaved and prepped in a sterile fashion. Following a lower abdominal midline incision, scaffolds were wrapped in the epididymal fat and returned to the intraperitoneal cavity. The abdominal wall was then closed with a running stitch, and the skin was closed with wound clips.

Flow cytometry

The following antibodies were purchased from Biolegend: anti-CD45 clone 30-F11; anti-CD8a clone 53-6.7; anti-Ly6G clone 1A8; anti-F4/80 clone BM8; anti-NK1.1 clone PK136, anti-CD19 clone 6D5, anti-I-A/I-E (MHCII) clone M5/114.15.2, and anti-CD16/32 clone 93. The following antibodies were purchased from eBioscience: anti-CD11b clone M1/70, anti-CD11c clone N418, and anti-Foxp3 clone FJK-16s. Anti-CD4 clone RM4-5 was purchased from BD Biosciences.

Following euthanization, scaffolds were harvested and immediately washed in ice cold Hanks Balanced Salt Solution (HBSS; Life Technologies). Excess tissue was trimmed such that only the immediate scaffold environment and integrated tissue were analyzed. Scaffolds were minced and incubated in collagenase (Roche) at 37°C for 20 min. The solution was then passed through a 70 μm filter, washed in PBS, and suspended in PBS containing anti-CD16/32 and LIVE/DEAD blue fixable dye (Life Technologies). Antibodies against extracellular antigens were then added. After extracellular antibody incubation, cells were washed to remove unbound antibody, fixed in fixation buffer (Biolegend) and analyzed on an LSRFortessa flow cytometer (BD Biosciences). The entire cellular infiltrate isolated from the scaffold and integrated tissue was analyzed by flow cytometry so the total number of immune cells could be reported. Data was analyzed in FlowJo software (Treestar). Isotype controls were used to set gates for immunophenotyping. Foxp3 was detected using eBioscience's Foxp3/Transcription factor staining buffer set.

The gating scheme for flow cytometry data is depicted in Supplemental Figure 1. Cellular events were gated using forward scatter and side scatter. Viable leukocytes were then identified by CD45 expression and low signal from viability stain, while cell aggregates were excluded with side scatter width. Ly6G and F4/80 positive cells were then identified. Cells negative for Ly6G and F4/80 were then gated for expression of CD4 and CD8. Cells negative for CD4 and CD8 were then gated for CD19 and NK1.1. Cells negative for CD19 and NK1.1 were gated for CD11b and CD11c.

Measuring cytokine expression within scaffolds

Following euthanization, scaffolds were harvested, washed in ice cold HBSS, and frozen using liquid nitrogen. Tissue was weighed and then homogenized in 500 μL of PBS containing Halt Protease Inhibitor Cocktail (Pierce) using a Dounce tissue grinder. Insoluble

material was removed by centrifugation, and samples were frozen using liquid nitrogen and stored at −80°C until use. All cytokines were measured using DuoSet® ELISA Kits (R&D Systems) as per the manufacturer's instructions.

Animals and induction of diabetes

Male C57BL/6 mice (Jackson Labs) between 8 and 12 weeks of age were used for syngeneic islet transplants. In allogeneic transplants, male BALB/c (Jackson Labs) and C57BL/6 mice between 8 and 12 weeks of age were used as islet donors and transplant recipients, respectively. Clinical diabetes was induced by intraperitoneal injection of 190 mg/kg of streptozotocin (Sigma). Diabetes was confirmed by blood glucose measurements greater than 300 mg/dL on two consecutive days prior to transplantation. The Northwestern University Animal Care and Use Committee approved all studies.

Islet isolation, scaffold seeding, and transplantation

Islet isolation and scaffold seeding were performed as previously described [19]. Briefly, islets were isolated from donor pancreata by a mechanically enhanced enzymatic digestion using collagenase (type XI; Sigma). After filtration through a mesh screen, the filtrate was applied to a discontinuous ficoll gradient (Sigma). Islets were handpicked from the gradient, washed, and counted. Scaffolds were immersed in 70% ethanol and then washed in serum-containing media. Each scaffold was seeded with 250 manually counted islets in a minimal volume of media by applying them to a single side of the scaffold and allowing them to settle onto the microporous structure. Examination of the tissue culture media following removal of the scaffolds demonstrated that greater than 98% of the islets were retained within the scaffolds. Prior to transplant, recipient mice were anesthetized with an intraperitoneal injection of ketamine (10 mg/kg) and xylazine (5 mg/kg), and the abdomen was shaved and prepped in a sterile fashion. For each recipient, following a lower abdominal midline incision, an islet-seeded scaffold was wrapped in the right epididymal fat pad and returned to the intraperitoneal cavity. The abdominal wall was then closed with a running stitch, and the skin was closed with wound clips.

Assessment of graft function

To assess graft function, non-fasting blood glucose measurements were taken between 12:00 and 17:00 after transplantation. Graft rejection was confirmed by two consecutive measurements of blood glucose levels more than 250 mg/dL.

Statistics

Multiple groups were compared using one-way ANOVA with the Tukey post-hoc test. Comparisons between two groups were made with an unpaired *t* test. Comparisons between two groups overtime were made using a two-way ANOVA with Bonferroni's multiple comparison test. The log-rank test was used to compare Kaplan-Meyer survival curves depicting islet survival. The specific test and information on the number of animals and experiments are specified in each figure legend. All analysis was carried out using GraphPad Prism. In all figures, error bars denote SEM.

Results

Scaffold structure and protein release

A layered scaffold design was implemented to facilitate incorporation of protein, while retaining an interconnected open-pore structure suitable of cell transplantation [20]. The scaffold consisted of a thin, non-porous center layer of PLG sandwiched between two porous outer layers of PLG (Fig. 1A). Fusion of the microspheres within the composite structure by gas foaming resulted in an effective union of the adjacent layers that withstood salt leaching and surgical implantation. Importantly, the outer layers have a porous structure that allows for effective islet transplantation, and the inner layer can be separately designed for sustained protein release.

We initially characterized the release profile of the TGF-β1 from scaffolds *in vitro* (Fig. 1B) as a prelude to investigating the immune response *in vivo*. Leaching of salt to remove the porogen resulted in loss of 13% of the TGF-β1 (data not shown). Of the remaining protein, 83% was released in the first day, with an additional 10% of the TGF-β1 released between days 1 and 3. The amount of TGF-β1 released after day 3 accounted for 7% of the total protein loaded into the center layer of the scaffold.

Leukocyte infiltration into TGF-β1 scaffolds

Initial *in vivo* studies investigated the leukocyte populations that infiltrate and reside within TGF-β1 loaded scaffolds following implantation. Flow cytometric analysis indicated that the number of leukocytes (identified by CD45 expression) within the scaffold 7 days after implantation was decreased in a dose dependent manner in response to TGF-β1 delivery. Scaffolds loaded with 0.2 μg and 2 μg of TGF-β1 contained 35% and 60% fewer leukocytes respectively, compared to scaffolds without TGF-β1 (Fig. 2A). Numbers of CD45 cells isolated from 2ug TGF-β1 scaffolds and control scaffolds were similar for 7 and 14 days after implantation (Sup. Fig 2).

We next investigated specific immune lineages residing in the scaffold after 7 days. Eight leukocyte populations were identified within the scaffolds, which were F4/80 macrophages, Ly6G neutrophils, CD11c DCs, CD11b monocytes, CD4 T cells, CD8 T cells, CD19 B cells, and NK1.1 NK cells (Fig. 2B). Significant decreases in the numbers of all leukocyte populations studied were observed at the 2 μg dose relative to the empty scaffold control, with the 0.2 μg dose exhibiting average values intermediate between the control and 2 μg dose. Notably F4/80 macrophages and NK1.1 NK cells exhibited a reduction of more than 69% and 74%, respectively, within the scaffold for the 2 μg dose relative to the no protein control. Despite the known role of TGF-β1 in generating Tregs through expression of Foxp3, there was a decrease in the number of Tregs in TGF-β1 scaffolds compared to the control scaffolds (Sup. Fig. 3); however, there was an increase in the expression level of Foxp3 amongst Tregs in scaffolds loaded with 2 μg of TGF-β1.

Leukocyte activity within TGF-β1 scaffolds

The activation status of antigen presenting cells (APCs) within the scaffold was investigated by measurement of MHCII expression by flow cytometry; activated cells are expected to

express higher levels of MHCII (Fig. 3A). F4/80 cells exhibited decreased MHCII surface expression within scaffolds loaded with 0.2 μg or 2 μg TGF-β1 scaffolds (20% and 30%, respectively) relative to control scaffolds. CD11c cells exhibited a 15% decrease in MHCII expression within scaffolds loaded with 2 μg of TGF-β1 compared to control scaffolds. In contrast, MHCII expression was not affected on CD11b cells. Ly6G cells, which do not typically express MHCII, were included as a control and did not stain positively for MHCII.

The significant decrease in leukocyte numbers and MHCII expression on APCs led to investigating cytokine and chemokine expression (Fig. 3B). At day 3, the NK cell chemokine CXCL10 and monocyte/macrophage chemokine MCP-1 were in highest abundance in scaffolds without TGF-β1. These factors exhibited a 53% and 47% decrease with TGF-β1 delivery, respectively. The T cell chemokine CCL5 was also decreased by 67%. TGF-β1 delivery decreased inflammatory cytokines TNF-a and IL-12 by 65% and 61%, respectively, while IL-1β exhibited a decreasing trend. Interestingly, expression of the anti-inflammatory cytokine IL-10 was also significantly decreased following TGF-β1 delivery. IFN- expression, if present, was below the level of detection (31 pg/mL).

Syngeneic islet transplant on TGF-β1 releasing scaffolds

The ability of localized TGF-β1 delivery to enhance islet function was initially investigated by seeding syngeneic islets isolated from healthy C57Bl/6 mice onto scaffolds containing 2 μg of TGF-β1 that were then implanted into male C57Bl/6 mice rendered diabetic by streptozotocin injection. Blood glucose was monitored daily to assess islet function (Fig. 4A). Islets transplanted on scaffolds containing 0 or 2 μg of TGF-β1 maintained similar blood glucose levels for the first three days after transplant. However, between days 4 and 6, islets transplanted on TGF-β1 scaffolds maintained significantly lower blood glucose levels. Following day 6, daily blood glucose levels for the two groups were not different for the remainder of the study. Tissue infiltration into the scaffold and vascularization were studied at day 7 post-transplant. Hematoxylin and eosin stained sections indicated greater host tissue integration around the central layer of the scaffold in the presence of TGF-β1 (Sup. Fig. 4); however, we did not observe differences in CD31+ staining of endothelial cells between the two groups (Sup. Fig. 5).

The ability of the engrafted islets to clear glucose from the circulation was investigated using an intraperitoneal glucose tolerance test that was performed at day 70. At this time point, no significant difference in the area under the curve was observed between the two groups (Fig. 4B). Finally, at day 80, the fat pads containing islets were removed. Within 4 days, all mice in both groups reverted to hyperglycemia (Fig. 4A), indicating that euglycemia was due to islet transplantation and not regeneration of endogenous islets.

Allogeneic islet transplant on TGF-β1 releasing scaffolds

The protection of allogeneic islets from immune rejection by localized delivery of TGF-β1 delivery was subsequently investigated. Islets isolated from healthy Balb/C mice were seeded onto TGF-β1 or empty control scaffolds and transplanted into diabetic C57Bl/6 mice. Two consecutive blood glucose measurements above 250 mg/dL indicated graft rejection. Kaplan-Meyer survival analysis of the two groups indicated that islets transplanted on TGF-

β1 scaffolds functioned significantly longer than those transplanted on empty controls (19 versus 12 days, respectively) (Fig 5).

Leukocyte infiltration into allogeneic islet transplants

The mechanism for extended allogeneic islet survival with TGF-β1 scaffolds was investigated by performing flow cytometry on allografts 7 days after transplant, a time that immediately preceded graft failure for the control scaffolds (Fig. 5). In the presence of TGF-β1, grafts exhibited 30% less CD45 cells compared to grafts without TGF-β1 (Fig 6A). Flow cytometry indicated that the numbers of F4/80 macrophages, CD11c DCs, and NK1.1 NK cells were significantly decreased by 70%, 45%, and 45%, respectively, in grafts delivering TGF-β1 relative to control (Fig 6B). However, both CD4 and CD8 T cells numbers were unaffected by TGF-β1 delivery. As observed previously in the blank implantations, the overall number of Tregs within the scaffold decreased with TGF-β1 delivery (Sup. Fig. 6). Additionally, we did not see an increase in the expression level of Foxp3 in the CD4 Foxp3 population.

The spatial distributions of key leukocyte populations were investigated within allogeneic islet transplants through immunofluorescence imaging of histological sections for scaffolds releasing TGF-β1 (Fig. 7 D–F) and control scaffolds (Fig. 7 A–C). In the absence of TGF-β1, F4/80 (Fig. 7A) and NK1.1 (Fig. 7B) signal was detected throughout the scaffold and around the islets. In contrast, in the presence of TGF-β1, F4/80 (Fig. 7D) and NK1.1 (Fig. 7E) signals were primarily localized to the exterior surface of the scaffold. However, TGF-β1 delivery failed to modulate CD8 T cell infiltration into the scaffold and amongst the islets (Fig. 7C versus Fig. 7F).

Discussion

This report investigated the delivery of TGF-β1 as a means to modulate inflammation following surgical implantation of PLG scaffolds. TGF-β1 delivery from scaffolds has been used to promote bone and cartilage regeneration *in vitro* [26–29] and *in vivo* [30–32]. Herein we demonstrate that scaffold-based delivery of TGF-β1 suppresses the local inflammatory response. TGF-β1 was delivered from layered scaffolds, where protein was entrapped within a solid PLG-mannitol inner layer and surrounded by a porous PLG outer layer designed for cell seeding and tissue engraftment. This scaffold design maintained TGF-β1 bioactivity and provided short-term release that was able to decrease leukocyte infiltration and inflammatory cytokine production within the implant. Functionally, the TGF-β1 scaffolds promoted better blood glucose control of syngeneic islets immediately after engraftment, and delayed rejection of allogeneic islets in diabetic mice. These findings are significant because inflammation following cell transplantation contributes to transplanted cell dysfunction or death.

TGF-β1 loaded scaffolds, in the absence of transplanted cells, reduced the infiltration of immune cells after implantation. All eight innate and adaptive immune cell types we identified by flow cytometry showed reduced populations within isolated TGF-β1 scaffolds. The decrease in infiltration of these cell types was dose-dependent, with the most significant decreases observed with delivery of 2 μg TGF-β1. Though TGF-β1 can serve as either a pro-

or anti-inflammatory stimulus depending on the local microenvironment [33], our model indicated TGF-β1 delivery has primarily immunosuppressive effects. While some reports have described TGF-β1's role as a monocyte and macrophage chemoattractant [34, 35], we observed significant decreases in these same myeloid lineage cells that suggests protein delivery blocks migration of these populations or inhibits their local proliferation. TGF-β1 is also known to promote immature and tolerogenic phenotypes on APCs [16, 37–39], which is consistent with the observed decreases in MHCII expression on APC populations. Despite the *in vitro* release assay data indicating that the majority of TGF-β1 was released within the initial 3 days, leukocyte infiltration was reduced for up to 14 days (Sup. Fig 2). Thus, short-term release of TGF-β1 has relatively long-term affects on leukocyte infiltration into the implant site.

TGF-β1 loaded scaffolds reduced expression of inflammatory cytokines within the adipose tissue 3 days after implant, which likely contributed to the reduced leukocyte infiltration at 7 days. Macrophages are the most abundant leukocyte in the adipose tissue [40] and their adhesion to biomaterials can induce activation [41, 42]. Activated macrophages release inflammatory mediators (e.g., TNF-a and IL-1β) that induce adipocytes and stromal vascular cells to release chemokines that recruit additional leukocytes. Indeed, the most abundant factors measured in the surrounding tissue three days after scaffold implantation were the chemokines MCP-1 and CXCL10, which were each decreased by 50% with delivery of TGF-β1. MCP-1 is recognized by CCR2, which is highly expressed on inflammatory monocytes that differentiate into macrophages and DCs after they exit the blood stream [43]. CXCL10 is a chemokine produced by monocytes, macrophages, and fibroblasts upon inflammatory stimulation that attracts T cells, B cells, and NK cells, which contribute to the rejection of allogeneic tissue [44]. High levels of both MCP-1 and CXCL10 have been found to correlate with graft failure and rejection [44, 45]. We also noted reductions in IL-12, TNF-a, and CCL5, which are inflammatory cytokines that potentiate transplant rejection through activation of APCs, polarization of naïve T cells towards a graft-destructive T_h1 effector phenotype, and migration of T cells to sites of inflammation [46, 47]. IL-10 expression was decreased in the presence of TGF-β1 delivery, likely due to the lower levels of inflammatory cytokines. Elevated expression of inflammatory cytokines has been reported to increase IL-10 expression by many leukocytes and other cell types and is thought to be a protective mechanism to control aberrant inflammation and damage to the host tissue [48].

Immediately after transplant, syngeneic islets on TGF-β1 releasing scaffolds were more effective at controlling blood glucose levels relative to islets on control scaffolds. While both scaffold types effectively reversed diabetes, we observed significantly lower blood glucose levels on days 4–6 post-surgery in mice receiving TGF-β1 releasing scaffolds. Since TGF-β1 has been reported to decrease islet insulin secretion [49] and vascularization of the scaffold at day 7 was not observed (Sup. Fig. 3), which could be indicative of TGF-β1 induced angiogenesis [50], we suggest that improved islet functionality is due to a more immunologically permissive microenvironment created by TGF-β1 delivery. Syngeneic or autologous cells can be damaged by nonspecific innate immunity [51]. Isolation and culture-related cell injury, ischemic reperfusion, or foreign body responses, can contribute to a local

inflammatory environment that damages the auto- or isograft during the initial engraftment period [52, 53]. Reduction of inflammatory cells and cytokines with TGF-β1 delivery within the peri-islet environment may prevent host-induced damage and enable more efficient engraftment that leads to superior function at early times. Importantly, maintenance of long-term euglycemia by syngeneic islets, as evidenced by daily blood glucose measurements and a glucose tolerance test conducted at day 70, confirmed that elevated local concentration of TGF-β1 at the time of implant did not deter islet graft viability or functionality, which is a frequent concern when testing immunosuppressive agents.

TGF-β1 delivery from the scaffolds delayed the rejection of transplanted allogeneic islets. Transplantation of allogeneic cells enhanced the severity of the local immune response, which was observed by the 67% increase in leukocyte infiltration compared to scaffold implantation alone (Fig 2A versus Fig 6A). The overall effect of TGF-β1 release on leukocyte infiltration was dampened in the allotransplants, where a 30% reduction in leukocytes was observed compared to 60% in scaffolds implanted without cells. There was a profound shift in the composition of infiltrating leukocytes towards lymphocytes, in particular CD8 T cells and NK cells, underscoring their role in allograft rejection. Significant decreases in the peri-islet innate immune cell populations (F4/80 macrophages, NK1.1 NK cells, CD11c DCs) were observed with TGF-β1 loaded scaffolds at day 7, which indicate innate leukocyte populations were still affected by protein release. These cell populations play significant roles in allograft rejection, thus delaying their arrival likely contributed to the delay in rejection. Macrophages act as both recruiters of inflammatory cell types and effectors of T cell-mediated graft destruction through the release of cytokines and reactive oxidative species [52, 54, 55]. DCs are the primary APC stimulating T cell proliferation and are a common therapeutic target to prevent allograft rejection [56]. Recent work has shown monocytes specifically recognize allogeneic tissue and preferentially differentiate into activated DCs that upregulate inflammatory cytokines compared to syngeneic tissue [57]. Finally, while NK cells may be required for induction of allograft tolerance through inhibition of T cell proliferation and destruction of graft-derived APCs [58], they also demonstrate the ability to eliminate allogeneic cells lacking self MHC-I molecules [59].

While TGF-β1 delivery delayed innate cell infiltration into allogeneic islet-containing scaffolds, CD4 or CD8 T cell populations did not show significant differences at day 7. Since T cells are the primary mediators of allograft rejection [60], we suggest that the 1-week extension in allograft survival seen with TGF-β1 delivery may be due to a delay in the full activation of infiltrating T cells. TGF-β1 can have suppressive effects on the priming of T cells [17, 18], and its release from the scaffold may provide a short-term stimulus that influences T cell activation. Additionally, considering the ability of CD4 T cells to express cytokines that can polarize macrophages toward inflammatory phenotypes [61], the decrease in overall macrophage population caused by the TGF-β1 scaffolds may have dampened a key effector mechanism of the CD4 T-cell response. While TGF-β1 is known to induce Foxp3 expression in CD4 T cells and may assist in the generation of peripheral Treg populations [18], we did not observe an increase in the induction of Tregs in the scaffolds in either the blank or allogeneic transplantation models (Sup. Figs 3 and 6). There was also no detectable increase in Foxp3 expression in Tregs present in scaffolds transplanted with

islets. Thus, it is unlikely that improvements in graft function were due to a TGF-β1 induced enhancement of local Treg populations. Thus, we believe the delay in rejection of allogeneic islets transplanted on TGF-β1 loaded scaffolds may have been caused by the decreased initial nonspecific damage from innate immune cell populations and a delay in the fully activated T cell response in the graft environment. Even though transient TGF-β1 release did not result in long-term allograft survival, we hypothesize that the profound reduction in inflammation demonstrated in this study could be used in combination with a system for long-term delivery or tolerance induction, such as nanoparticle alloantigen delivery to non-activated APCs [62], in order to promote long-term allograft survival.

Conclusions

Scaffolds designed to release recombinant TGF-β1 elicited less inflammation after implant by decreasing local cytokine concentrations and leukocyte infiltration. This immunomodulated scaffold transplant environment supported better islet function and longer islet survival in syngeneic and allogeneic models of islet transplant, respectively. Analysis of leukocyte infiltration into allogeneic grafts revealed significant decreases in innate immune cell lineages, suggesting that extended allograft survival on TGF-β1 scaffolds could be linked to reductions in nonspecific tissue damage and a delay in the full T cell response. This approach for locally controlling inflammation after biomaterial implantation may enhance systemic strategies for tolerance induction in order to promote engraftment and long-term function of allogeneic transplants.

Supplementary Material

Refer to Web version on PubMed Central for supplementary material.

Acknowledgments

Financial support for this research was provided by the National Institutes of Biomedical Imaging and Bioengineering (NIBIB) at the National Institutes of Health (NIH) through grant number R01 EB009910, R01 EB005678, and R01 CA173745, the National Institute of General Medical Sciences at the NIH through grant numbers P20 GM103641 and T32 GM008449, and the Juvenile Diabetes Research Foundation. This work was also supported by the Northwestern University RHLCCC Flow Cytometry Facility and a Cancer Center Support Grant (NCI CA060553).

References

1. Sanganalmath SK, Bolli R. Cell therapy for heart failure: a comprehensive overview of experimental and clinical studies, current challenges, and future directions. Circulation research. 2013; 113:810–34. [PubMed: 23989721]
2. Forbes SJ, Gupta S, Dhawan A. Cell therapy for liver disease: From liver transplantation to cell factory. Journal of hepatology. 2015; 62:S157–S69. [PubMed: 25920085]
3. Aboody K, Capela A, Niazi N, Stern JH, Temple S. Translating stem cell studies to the clinic for CNS repair: current state of the art and the need for a Rosetta stone. Neuron. 2011; 70:597–613. [PubMed: 21609819]
4. Cogger K, Nostro MC. Recent advances in cell replacement therapies for the treatment of type 1 diabetes. Endocrinology. 2015; 156:8–15. [PubMed: 25386833]
5. Li YS, Harn HJ, Hsieh DK, Wen TC, Subeq YM, Sun LY, et al. Cells and materials for liver tissue engineering. Cell transplantation. 2013; 22:685–700. [PubMed: 23127824]

6. Segers VF, Lee RT. Biomaterials to enhance stem cell function in the heart. Circulation research. 2011; 109:910–22. [PubMed: 21960724]
7. Orive G, Anitua E, Pedraz JL, Emerich DF. Biomaterials for promoting brain protection, repair and regeneration. Nature reviews Neuroscience. 2009; 10:682–92. [PubMed: 19654582]
8. Kolaczkowska E, Kubes P. Neutrophil recruitment and function in health and inflammation. Nature reviews Immunology. 2013; 13:159–75.
9. Rocha PN, Plumb TJ, Crowley SD, Coffman TM. Effector mechanisms in transplant rejection. Immunological reviews. 2003; 196:51–64. [PubMed: 14617197]
10. Heeger PS. T-cell allorecognition and transplant rejection: a summary and update. American journal of transplantation : official journal of the American Society of Transplantation and the American Society of Transplant Surgeons. 2003; 3:525–33.
11. Roake JA, Austyn JM. The role of dendritic cells and T cell activation in allograft rejection. Experimental nephrology. 1993; 1:90–101. [PubMed: 8081962]
12. Clatworthy MR. B cell responses to allograft--more common than we thought? American journal of transplantation : official journal of the American Society of Transplantation and the American Society of Transplant Surgeons. 2013; 13:1629–30.
13. Stolp J, Turka LA, Wood KJ. B cells with immune-regulating function in transplantation. Nature reviews Nephrology. 2014; 10:389–97. [PubMed: 24846332]
14. Zeng Q, Ng YH, Singh T, Jiang K, Sheriff KA, Ippolito R, et al. B cells mediate chronic allograft rejection independently of antibody production. The Journal of clinical investigation. 2014; 124:1052–6. [PubMed: 24509079]
15. Yang L, Pang Y, Moses HL. TGF-beta and immune cells: an important regulatory axis in the tumor microenvironment and progression. Trends in immunology. 2010; 31:220–7. [PubMed: 20538542]
16. Kobie JJ, Wu RS, Kurt RA, Lou S, Adelman MK, Whitesell LJ, et al. Transforming growth factor beta inhibits the antigen-presenting functions and antitumor activity of dendritic cell vaccines. Cancer research. 2003; 63:1860–4. [PubMed: 12702574]
17. Bonham CA, Lu L, Banas RA, Fontes P, Rao AS, Starzl TE, et al. TGF-beta 1 pretreatment impairs the allostimulatory function of human bone marrow-derived antigen-presenting cells for both naive and primed T cells. Transplant immunology. 1996; 4:186–91. [PubMed: 8893447]
18. Fu S, Zhang N, Yopp AC, Chen D, Mao M, Chen D, et al. TGF-beta induces Foxp3 + T-regulatory cells from CD4 + CD25 − precursors. American journal of transplantation : official journal of the American Society of Transplantation and the American Society of Transplant Surgeons. 2004; 4:1614–27.
19. Blomeier H, Zhang X, Rives C, Brissova M, Hughes E, Baker M, et al. Polymer scaffolds as synthetic microenvironments for extrahepatic islet transplantation. Transplantation. 2006; 82:452–9. [PubMed: 16926587]
20. Gibly RF, Zhang X, Graham ML, Hering BJ, Kaufman DB, Lowe WL Jr, et al. Extrahepatic islet transplantation with microporous polymer scaffolds in syngeneic mouse and allogeneic porcine models. Biomaterials. 2011; 32:9677–84. [PubMed: 21959005]
21. Chen X, Zhang X, Larson C, Chen F, Kissler H, Kaufman DB. The epididymal fat pad as a transplant site for minimal islet mass. Transplantation. 2007; 84:122–5. [PubMed: 17627248]
22. Salvay DM, Rives CB, Zhang X, Chen F, Kaufman DB, Lowe WL Jr, et al. Extracellular matrix protein-coated scaffolds promote the reversal of diabetes after extrahepatic islet transplantation. Transplantation. 2008; 85:1456–64. [PubMed: 18497687]
23. Hlavaty KA, Gibly RF, Zhang X, Rives CB, Graham JG, Lowe WL Jr, et al. Enhancing human islet transplantation by localized release of trophic factors from PLG scaffolds. American journal of transplantation : official journal of the American Society of Transplantation and the American Society of Transplant Surgeons. 2014; 14:1523–32.
24. Harris LD, Kim BS, Mooney DJ. Open pore biodegradable matrices formed with gas foaming. Journal of biomedical materials research. 1998; 42:396–402. [PubMed: 9788501]
25. Gower RM, Boehler RM, Azarin SM, Ricci CF, Leonard JN, Shea LD. Modulation of leukocyte infiltration and phenotype in microporous tissue engineering scaffolds via vector induced IL-10 expression. Biomaterials. 2014; 35:2024–31. [PubMed: 24309498]

26. Chou CH, Cheng WT, Lin CC, Chang CH, Tsai CC, Lin FH. TGF-beta1 immobilized tri-copolymer for articular cartilage tissue engineering. Journal of biomedical materials research Part B, Applied biomaterials. 2006; 77:338–48.
27. Holland TA, Tabata Y, Mikos AG. Dual growth factor delivery from degradable oligo(poly(ethylene glycol) fumarate) hydrogel scaffolds for cartilage tissue engineering. Journal of controlled release : official journal of the Controlled Release Society. 2005; 101:111–25. [PubMed: 15588898]
28. Kim SE, Park JH, Cho YW, Chung H, Jeong SY, Lee EB, et al. Porous chitosan scaffold containing microspheres loaded with transforming growth factor-beta1: implications for cartilage tissue engineering. Journal of controlled release : official journal of the Controlled Release Society. 2003; 91:365–74. [PubMed: 12932714]
29. Lee JE, Kim SE, Kwon IC, Ahn HJ, Cho H, Lee SH, et al. Effects of a chitosan scaffold containing TGF-beta1 encapsulated chitosan microspheres on in vitro chondrocyte culture. Artificial organs. 2004; 28:829–39. [PubMed: 15320946]
30. Cucchiarini M, Sohier J, Mitosch K, Kaul G, Zurakowski D, Bezemer J, et al. Effect of transforming growth factor-beta 1 (TGF-β1) released from a scaffold on chondrogenesis in an osteochondral defect model in the rabbit. centeurjbiol. 2006; 1:43–60.
31. Fan H, Hu Y, Qin L, Li X, Wu H, Lv R. Porous gelatin-chondroitin-hyaluronate tri-copolymer scaffold containing microspheres loaded with TGF-beta1 induces differentiation of mesenchymal stem cells in vivo for enhancing cartilage repair. Journal of biomedical materials research Part A. 2006; 77:785–94. [PubMed: 16575912]
32. Holland TA, Bodde EW, Cuijpers VM, Baggett LS, Tabata Y, Mikos AG, et al. Degradable hydrogel scaffolds for in vivo delivery of single and dual growth factors in cartilage repair. Osteoarthritis and cartilage/OARS, Osteoarthritis Research Society. 2007; 15:187–97.
33. Kubiczkova L, Sedlarikova L, Hajek R, Sevcikova S. TGF-beta - an excellent servant but a bad master. Journal of translational medicine. 2012; 10:183. [PubMed: 22943793]
34. Wahl SM, Hunt DA, Wakefield LM, McCartney-Francis N, Wahl LM, Roberts AB, et al. Transforming growth factor type beta induces monocyte chemotaxis and growth factor production. Proceedings of the National Academy of Sciences of the United States of America. 1987; 84:5788–92. [PubMed: 2886992]
35. Olieslagers S, Pardali E, Tchaikovski V, ten Dijke P, Waltenberger J. TGF-beta1/ALK5-induced monocyte migration involves PI3K and p38 pathways and is not negatively affected by diabetes mellitus. Cardiovascular research. 2011; 91:510–8. [PubMed: 21478266]
36. Kim JS, Kim JG, Moon MY, Jeon CY, Won HY, Kim HJ, et al. Transforming growth factor-beta1 regulates macrophage migration via RhoA. Blood. 2006; 108:1821–9. [PubMed: 16705092]
37. Geissmann F, Revy P, Regnault A, Lepelletier Y, Dy M, Brousse N, et al. TGF-beta 1 prevents the noncognate maturation of human dendritic Langerhans cells. Journal of immunology. 1999; 162:4567–75.
38. Gong D, Shi W, Yi SJ, Chen H, Groffen J, Heisterkamp N. TGFbeta signaling plays a critical role in promoting alternative macrophage activation. BMC immunology. 2012; 13:31. [PubMed: 22703233]
39. Leshansky L, Aberdam D, Itskovitz-Eldor J, Berrih-Aknin S. Human embryonic stem cells prevent T-cell activation by suppressing dendritic cells function via TGF-beta signaling pathway. Stem cells. 2014; 32:3137–49. [PubMed: 25186014]
40. Weisberg SP, McCann D, Desai M, Rosenbaum M, Leibel RL, Ferrante AW Jr. Obesity is associated with macrophage accumulation in adipose tissue. The Journal of clinical investigation. 2003; 112:1796–808. [PubMed: 14679176]
41. Jenney CR, Anderson JM. Adsorbed serum proteins responsible for surface dependent human macrophage behavior. Journal of biomedical materials research. 2000; 49:435–47. [PubMed: 10602077]
42. McNally AK, Jones JA, Macewan SR, Colton E, Anderson JM. Vitronectin is a critical protein adhesion substrate for IL-4-induced foreign body giant cell formation. Journal of biomedical materials research Part A. 2008; 86:535–43. [PubMed: 17994558]

43. Geissmann F, Jung S, Littman DR. Blood monocytes consist of two principal subsets with distinct migratory properties. Immunity. 2003; 19:71–82. [PubMed: 12871640]
44. Romagnani P, Crescioli C. CXCL10: a candidate biomarker in transplantation. Clinica chimica acta; international journal of clinical chemistry. 2012; 413:1364–73.
45. Agostini C, Calabrese F, Rea F, Facco M, Tosoni A, Loy M, et al. Cxcr3 and its ligand CXCL10 are expressed by inflammatory cells infiltrating lung allografts and mediate chemotaxis of T cells at sites of rejection. The American journal of pathology. 2001; 158:1703–11. [PubMed: 11337368]
46. Piccotti JR, Li K, Chan SY, Eichwald EJ, Bishop DK. Interleukin-12 (IL-12)-driven alloimmune responses in vitro and in vivo: requirement for beta1 subunit of the IL-12 receptor. Transplantation. 1999; 67:1453–60. [PubMed: 10385085]
47. Shen H, Goldstein DR. IL-6 and TNF-alpha synergistically inhibit allograft acceptance. Journal of the American Society of Nephrology : JASN. 2009; 20:1032–40. [PubMed: 19357252]
48. Saraiva M, O'Garra A. The regulation of IL-10 production by immune cells. Nature reviews Immunology. 2010; 10:170–81.
49. Lin HM, Lee JH, Yadav H, Kamaraju AK, Liu E, Zhigang D, et al. Transforming growth factor-beta/Smad3 signaling regulates insulin gene transcription and pancreatic islet beta-cell function. The Journal of biological chemistry. 2009; 284:12246–57. [PubMed: 19265200]
50. Ferrari G, Cook BD, Terushkin V, Pintucci G, Mignatti P. Transforming growth factor-beta 1 (TGF-beta1) induces angiogenesis through vascular endothelial growth factor (VEGF)-mediated apoptosis. Journal of cellular physiology. 2009; 219:449–58. [PubMed: 19180561]
51. Arita S, Une S, Ohtsuka S, Atiya A, Kasraie A, Shevlin L, et al. Prevention of primary islet isograft nonfunction in mice with pravastatin. Transplantation. 1998; 65:1429–33. [PubMed: 9645797]
52. Wood KJ, Goto R. Mechanisms of rejection: current perspectives. Transplantation. 2012; 93:1–10. [PubMed: 22138818]
53. Morais JM, Papadimitrakopoulos F, Burgess DJ. Biomaterials/tissue interactions: possible solutions to overcome foreign body response. AAPS J. 2010; 12:188–96. [PubMed: 20143194]
54. Wyburn KR, Jose MD, Wu H, Atkins RC, Chadban SJ. The role of macrophages in allograft rejection. Transplantation. 2005; 80:1641–7. [PubMed: 16378052]
55. Zecher D, van Rooijen N, Rothstein DM, Shlomchik WD, Lakkis FG. An innate response to allogeneic nonself mediated by monocytes. Journal of immunology. 2009; 183:7810–6.
56. Vassalli G. Dendritic cell-based approaches for therapeutic immune regulation in solid-organ transplantation. Journal of transplantation. 2013; 2013:761429. [PubMed: 24307940]
57. Oberbarnscheidt MH, Zeng Q, Li Q, Dai H, Williams AL, Shlomchik WD, et al. Non-self recognition by monocytes initiates allograft rejection. The Journal of clinical investigation. 2014; 124:3579–89. [PubMed: 24983319]
58. Beilke JN, Kuhl NR, Van Kaer L, Gill RG. NK cells promote islet allograft tolerance via a perforin-dependent mechanism. Nature medicine. 2005; 11:1059–65.
59. Liu W, Xiao X, Demirci G, Madsen J, Li XC. Innate NK cells and macrophages recognize and reject allogeneic nonself in vivo via different mechanisms. Journal of immunology. 2012; 188:2703–11.
60. Makhlouf L, Yamada A, Ito T, Abdi R, Ansari MJ, Khuong CQ, et al. Allorecognition and effector pathways of islet allograft rejection in normal versus nonobese diabetic mice. Journal of the American Society of Nephrology : JASN. 2003; 14:2168–75. [PubMed: 12874472]
61. Murray PJ, Wynn TA. Protective and pathogenic functions of macrophage subsets. Nature reviews Immunology. 2011; 11:723–37.
62. Bryant J, Hlavaty KA, Zhang X, Yap WT, Zhang L, Shea LD, et al. Nanoparticle delivery of donor antigens for transplant tolerance in allogeneic islet transplantation. Biomaterials. 2014; 35:8887–94. [PubMed: 25066477]

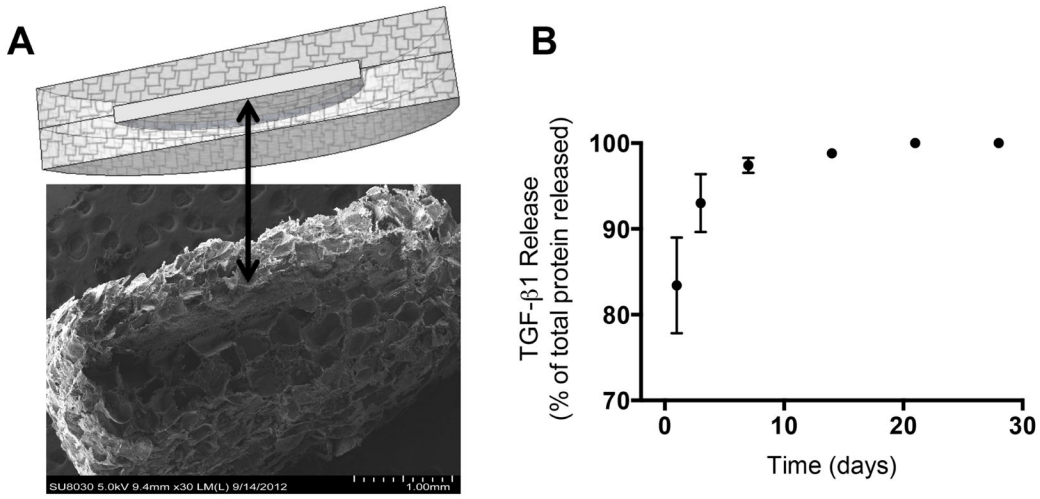

Fig 1. Scaffold microstructure and protein release profile

(A) Diagram and scanning electron microscope image of a layered scaffold. Black arrow indicates the protein-containing center layer. **(B)** *In vitro* release profile from five layered scaffolds containing 2μg of TGF-β1 as measured by ELISA.

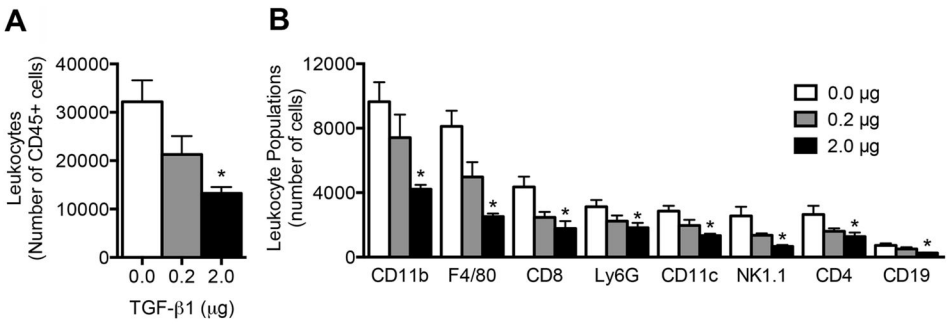

Fig 2. Leukocyte infiltration into TGF-β1 scaffolds

(A) Number of leukocytes isolated from TGF-β1 scaffolds seven days after implant as measured by flow cytometry. **(B)** Prevalence of leukocyte populations within TGF-β1 scaffolds. Data is from 8 scaffolds from 4 mice per condition receiving bilateral scaffold implants into the epididymal fat pads. * indicates $P < 0.05$ versus 0 μg. Statistics determined one-way ANOVA with Tukey's Multiple Comparison Test.

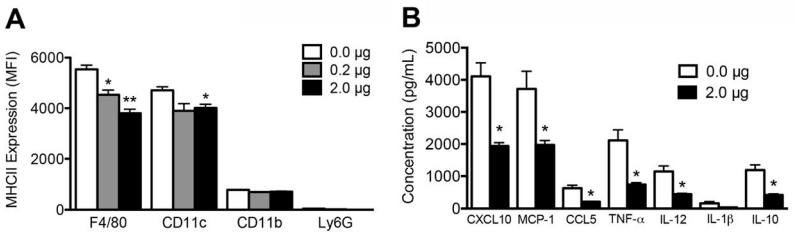

Fig 3. MHCII and cytokine expression within TGF-β1 scaffolds

(A) MHCII expression on leukocytes within scaffolds containing a dose range of TGF-β1 collected seven days after implant. Data is from 8 scaffolds per condition isolated from 4 mice receiving bilateral scaffold implants into the epididymal fat pads. * indicates $P < 0.05$ versus 0 µg. ** indicates $P < 0.05$ versus 0.2 µg. Statistics determined by one-way ANOVA with Tukey's Multiple Comparison Test. **(B)** Cytokines detected by ELISA in scaffold homogenate collected three days after implant. Data is from 10 scaffolds isolated from 5 mice per condition receiving bilateral scaffold implants into the epididymal fat pads. * indicates $P < 0.05$ versus 0.0 µg. Statistics determined by unpaired t-test.

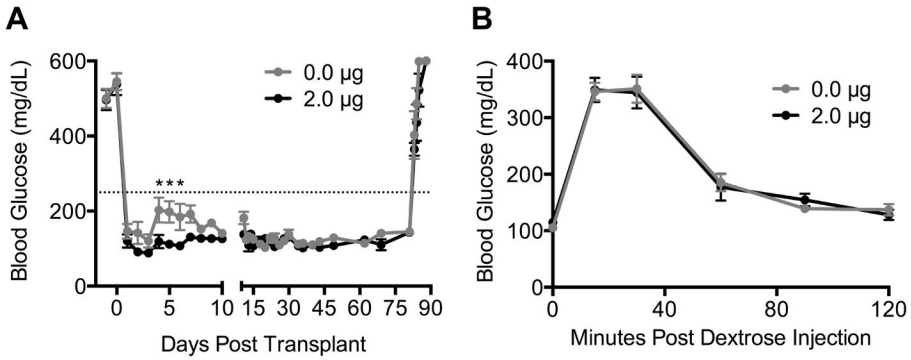

Fig 4. Syngeneic islet function on TGF-β1 scaffolds

(A) Blood glucose versus days post transplant for diabetic mice receiving syngeneic islet transplants on TGF-β1 scaffolds. Fat pads containing islets were removed at day 80. Dotted line indicates a blood glucose level of 250 mg/dL, and two consecutive readings above 250 would indicate graft failure. Data is from 8 scaffolds from 8 mice per condition receiving one scaffold implant into the right epididymal fat pad. * indicates $P < 0.05$ versus 0 µg on same day. Statistics determined by a two-way ANOVA with Bonferroni's multiple comparisons test. **(B)** Blood glucose versus time following an intraperitoneal dextrose injection. Glucose tolerance test was performed on day 70.

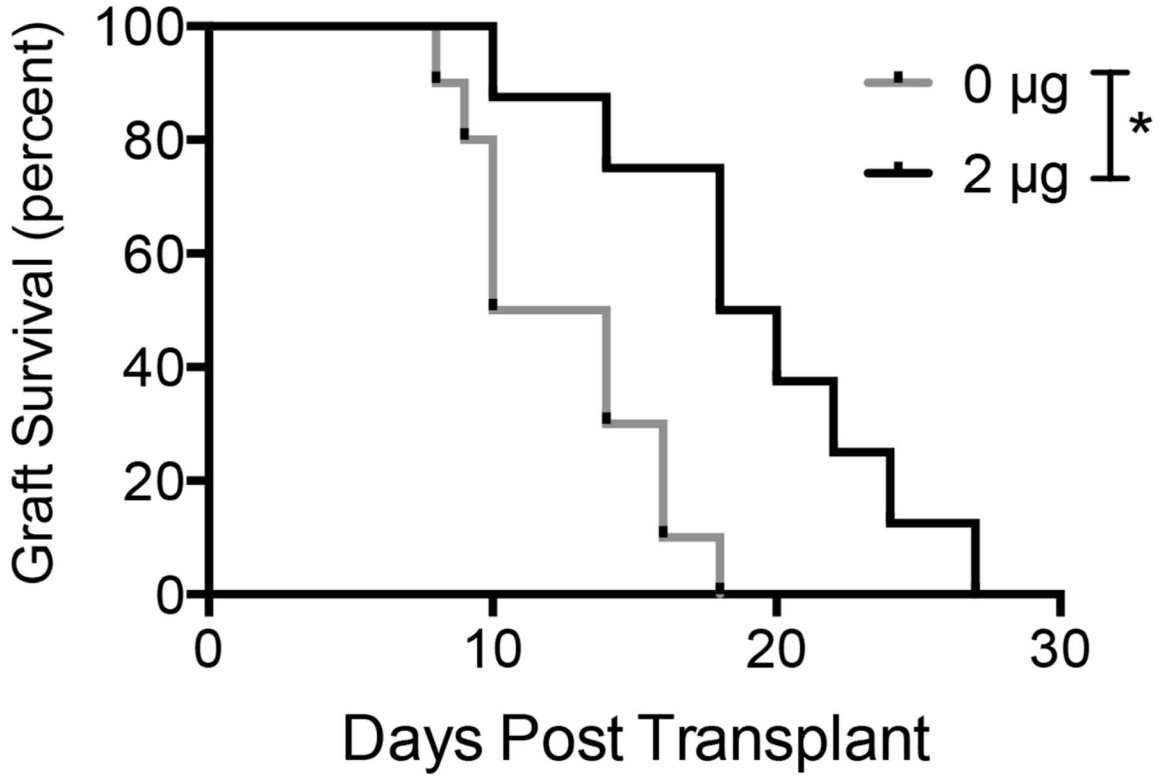

Fig 5. Allogeneic islet function on TGF-β1 scaffolds

Kaplan-Meyer survival curve of islet grafts versus time. Two consecutive blood glucose measurements above 250 mg/dL indicated graft failure. Data is from 8–10 mice receiving one scaffold implant into the right epididymal fat pad. * indicates $P < 0.01$. Statistics determined by log-rank test.

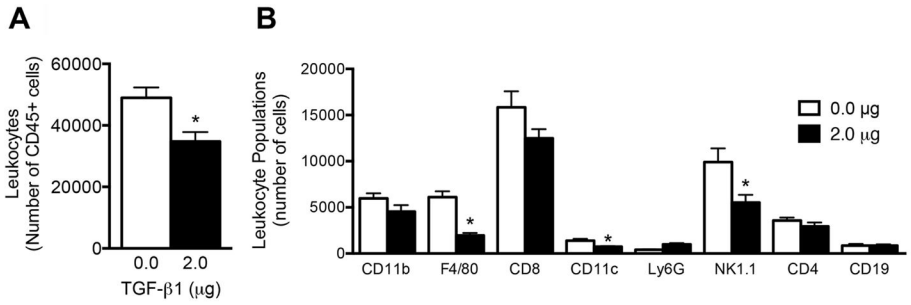

Figure 6. Leukocyte infiltration into allogeneic islet grafts implanted on TGF-β1 scaffolds

(A) Total number of CD45 positive cells isolated from islet allografts seven days after transplant. **(B)** Leukocyte populations within the islet allograft seven days after transplant. Data is from 7–9 scaffolds from 7–9 mice per condition receiving one scaffold implant into the right epididymal fat pad. * indicates $P < 0.05$. Statistics determined by unpaired t-test.

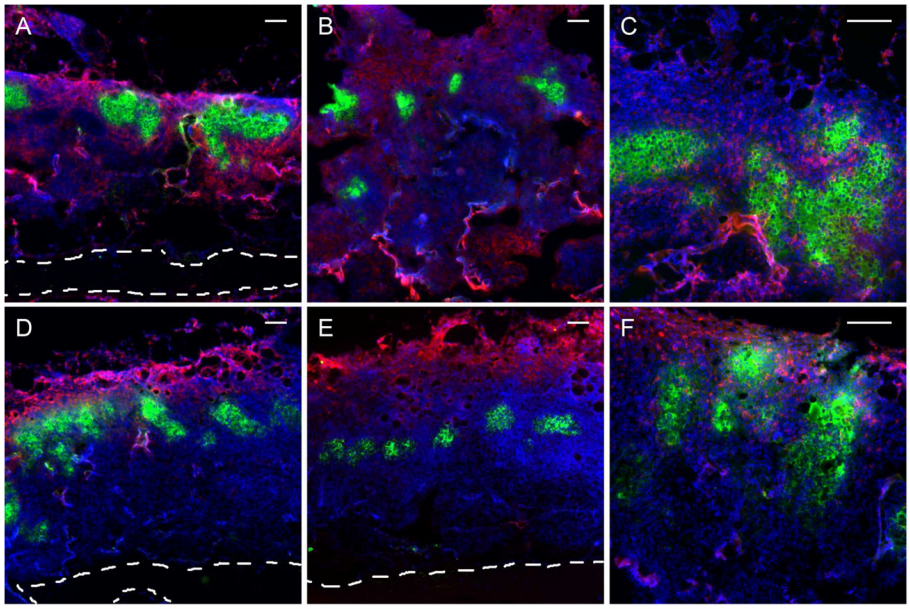

Figure 7. Immunofluorescence imaging of leukocyte infiltration into allogeneic islet grafts implanted on TGF-β1 scaffolds

Immunofluorescent detection of insulin (green), nuclei (blue) and **(A,D)** F4/80, **(B,E)** NK1.1, or **(C,F)** CD8 (red) within histological sections of islet grafts transplanted on scaffolds containing 0 μg (**A–C**) and 2 μg (**D–F**) of TGF-β1 at day seven. Scale bars located in the top right of each image indicate 100μm. Images representative of sections from 4 mice per condition.